Suspended Graphene Nanoribbon Ion-Sensitive Field-Effect Transistors Formed by Shrink Lithography for pH/Cancer Biomarker Sensing

Bo Zhang and Tianhong Cui, *Senior Member, IEEE*

***Abstract*—Low-cost and facile shrink lithography is utilized to form suspended graphene nanoribbon (GNR) for an ion-sensitive field-effect transistor (ISFET) with pH/cancer marker sensing applications. By combining shrink thermoplastic film with hot embossing process, GNR patterns 50 nm wide are achieved in a low-cost and simple way. Ambipolar characteristics of a suspended GNR ISFET after annealing presents an enhanced ambipolar effect. Different pH solutions are introduced to characterize the performance of GNR ISFET. For cancer biomarker sensing, the suspended GNR functionalized with specific anti-PSA antibodies as bio-receptor are capable of detecting prostate specific antigen down to 0.4 pg/mL. In comparison, the unsuspended GNR and microscale graphene sheet based ISFETs through the same design and fabrication are characterized under the same measurement conditions, showing that suspended GNR ISFET is superior in sensitivity and detection limit. [2012-0289]**

***Index Terms*—Graphene nanoribbon, ion-sensitive field-effect transistor, prostate-specific antigen, shrink lithography, suspended.**

I. Introduction

GRAPHENE nanoribbons (GNRs) are becoming an attractive nanostructure with a wealth of electrical, chemical, and mechanical properties [1]–[3]. Several GNR synthesis approaches were developed, including lithographic patterning [1], [4] and unzipping of carbon nanotubes [5]–[8]. Recently, GNR has been employed as a sensing material for the detection of biomolecules [9] with unique advantages due to its tunable ambipolar field-effect characteristics [3], relatively low 1/f noise, and biocompatibility [10]. However, investigation of the potential applications of GNR is greatly limited due to the complexity and high cost of these conventional synthetic methods, which require expensive equipment or complex procedures. Although some unconventional GNR fabrication methods were proposed to achieve a lower-cost and simple processes, such as nanosphere lithography [11], block copolymers assisted nanolithography [12], etc., there are still great efforts needed to satisfy the requirements for massive and low-cost fabrication of GNR. In the meanwhile, current studies have been focused on graphene attached on silicon oxide substrates [13]–[15]. However, charge traps at the interface and in the oxide have been reported as external scattering centers, and they degrade the electrical properties of graphene [16].

To overcome the previous hurdles of GNR research, an ion-sensitive field-effect transistor (ISFET), based on suspended GNR formed by shrink lithography, was proposed for applications to pH/cancer marker sensing. Herein, shrink lithography combines an embossing process of thermoplastic films to successfully achieve GNR patterns in a low-cost and simple way. Though thermoplastics have been used in microfabrication since 1998, the feature sizes of patterning are limited in microscale [17], [18]. Compared to traditional fabrication processes such as photolithography and electron beam lithography, the shrink lithography utilizes the embossing process of shrink materials with features including low cost, mass production, and good resolution. Due to the reusable mold of shrink lithography, this patterning process can further decrease the fabrication cost for GNR. To eliminate the effects from silicon oxide substrates, a suspended GNR structure is fabricated to decrease the electrical noise. With rational chemical modification, the suspended GNR ISFET is capable of detecting prostate-specific antigen (PSA). Its low electrical noise due to the suspended structure and annealing provide a promising approach to achieve a lower detection limit and a higher sensitivity.

Manuscript received October 1, 2012; revised February 3, 2013; accepted March 8, 2013. Date of publication May 13, 2013; date of current version September 27, 2013. The work was supported in part by the Minnesota Partnership sponsorship. Subject Editor C. H. Ahn.

The authors are with the Department of Mechanical Engineering, University of Minnesota, Minneapolis, MN 55455 USA (e-mail: tcui@me.umn.edu).

Color versions of one or more of the figures in this paper are available online at http://ieeexplore.ieee.org.

Digital Object Identifier 10.1109/JMEMS.2013.2254701

II. Design and Fabrication

A. Mold Fabrication and Shrink Lithography

The fabrication processes of the suspended GNR ISFET are illustrated in Fig. 1(a). First, a cleaned silicon wafer with SiO_2 300 nm thick was patterned by photolithography with photoresistance of Shipley S1813 about 1 mm thick spin-coated at 3,000 rpm for 30 s, and exposed for 6 s, followed by buffered HF (BOE 10:1) etching for 7 min. Next, the patterned wafer was etched by 20% KOH at 80 °C for 10 min, and the SiO_2 was the passivation layer. Next, chromium/gold layers 50/200 nm thick as a seed layer were deposited on the substrate by an AJA sputter system (Model ATC 2000). Nickel electroforming was conducted on a nickel plating station (SE-101, Digital Matrix Co., U.S.) using the patterned wafer as mandrel. A nickel sulfamate bath and a pulse reverse power were used to obtain uniform and stress free nickel mold. After

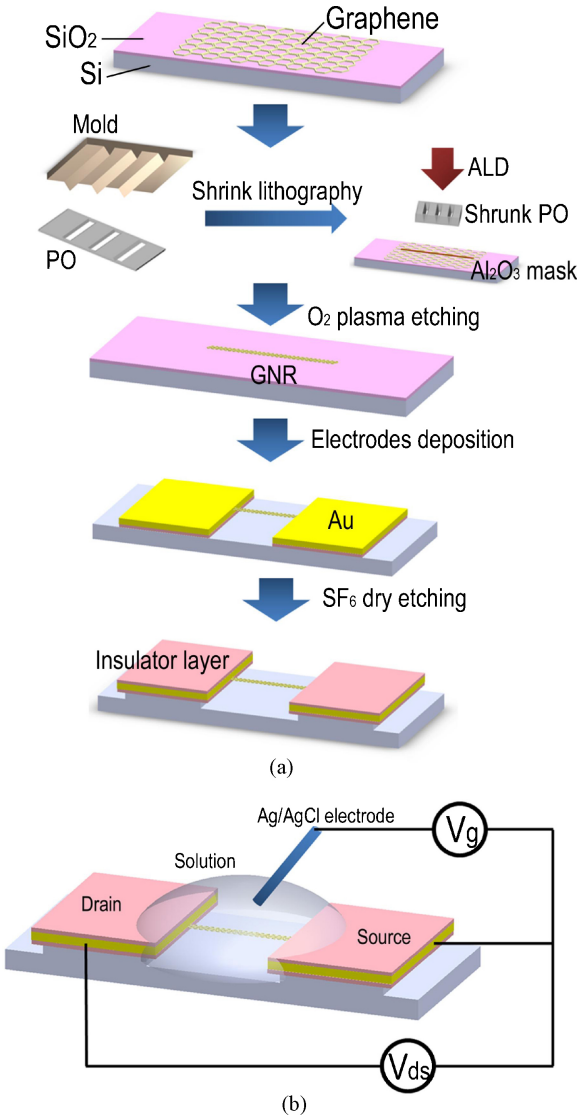

Fig. 1. (a) Schematic of the fabrication processes of suspended GNR by shrink lithography. (b) Schematic of suspended GNR ISFET.

electroforming, the silicon wafer was completely removed by 20% KOH at 80 °C. The obtained nickel mold was further cleaned by acetone and de-ionized water.

After the preparation of the mold, it was embossed against the shrink film under a press of 35 kN and held for 2 min by Maual Pressor (Model Grimco 12-1-HT). The shrink film (Sealed Air Nexcel multilayer shrink film 955D) comprising of five layers of co-extruded polyolefin (PO) was purchased from Sealed Air. Next, release the mold, and PO shrink film with impenetrated patterns was made. Sequentially, the patterned PO shrink film was placed between two silicon wafers for uniform heating, and heated to desired temperature of 15 °C in a slowly rising process for approximately 5 min and held for 10 min for shrinkage in a convection oven (Model 280A). As shown in Fig. 2, the impenetrated pattern in PO film shrunk greatly after applying heat. Due to the adhesion of shrink polymer film at high shrink temperature, the PO shrink film bonded with substrate very well, as the shadow mask for Al_2O_3 deposition.

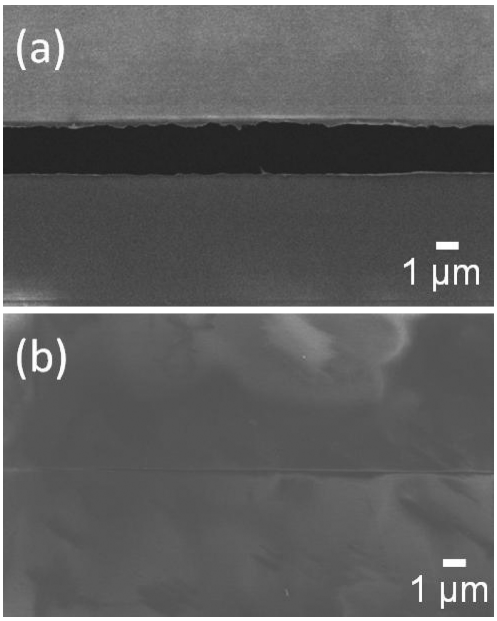

Fig. 2. SEM image of the shrink polymer PO with (a) non-shrink pattern and (b) shrunk pattern.

B. Manufacture of Suspended Graphene Nanoribbon Sensor

By using shrink lithography, extreme narrow impenetrated pattern was obtained on the PO shrink film. A layer of Al_2O_3 8 nm thick was deposited by atomic layer deposition (ALD), and the shrunk PO film was acting as a shadow mask. Next, the PO film was directly and gently stripped, and an Al_2O_3 nanoribbon was left as a mask on the graphene generated by mechanical exfoliation reported by our group [19]. The substrate was followed by oxygen plasma etching with STS etcher (Model 320, 10 s). The pre-patterned marks on the substrate assisted the alignment and location. After that, the substrate was immersed into KOH solution to remove the Al_2O_3 mask. Next, chromium/gold electrodes 50/200 nm thick were deposited on the two ends of graphene nanoribbon by an electron-beam evaporation (Model SEC 600), and metal lift-off. The SiO_2 layer 300 nm thick underneath graphene ribbons was etched away by buffered HF (BOE 10:1) for 7 min. Next, an Al_2O_3 layer was deposited to insulate the two electrodes. Finally, the suspended GNR structure was released by SF_6 dry etching of the silicon underneath with STS etcher (Model 320, 10 min).

The GNR was functionalized by immobilization of antibody on the surface. Due to the surface tension of water, the modification process was executed in aqueous solution all the time to keep the suspension structure. A suspended graphene nanoribbon sensor was first immersed into a 0.1% poly-l-lysine (Sigma-Aldrich Inc.) solution for 1 h at room temperature. The 0.1% poly-l-lysine is the adhesive layer to immobilize the anti-PSA. The poly-l-lysine is positively charged, attracting the negative charged anti-PSA to the GNR surface [20], [21]. Next, the biosensor was incubated for overnight at 4 ºC in anti-PSA capture antibody solution (Goat Polyclonal, BioCheck Inc.) at a concentration of 10 μg/mL prepared by a dilution into PBS (Dulbecco's phosphate buffered saline, Invitrogen

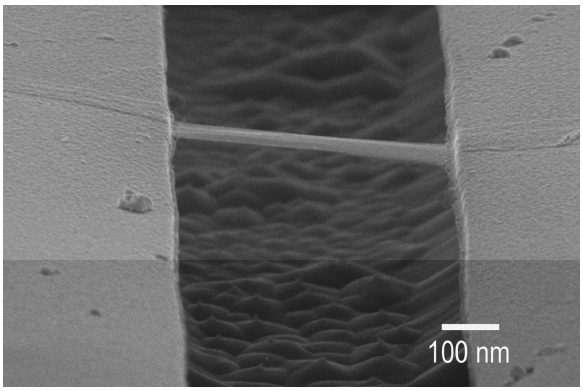

Fig. 3. SEM image of the suspended GNR structure before modification of anti-PSA. The width of the GNR is about 50 nm.

Inc.). The sensor was then immersed in a PBS solution for 10 min to rinse the biosensors. Next, the sensor was incubated in 3% bovine serum albumin blocking solution (Sigma-Aldrich Inc.) at room temperature for 5 h to block nonspecific binding sites. After repeating the rinsing step, the label free sensor was ready for testing.

In the target detection experiments, a target solution was added into the recording chamber, in which an Ag/AgCl reference electrode (EE008, Cypress systems Inc.) was immersed to apply a desired gate voltage, as shown in Fig. 1(b). While the ISFET was biased at $V_{ds} - 1$ to 1 V, the gate voltage was applied at -1.8 to 1.8 V. Electrical measurements were carried out using a semiconductor analyzer (HP 4145B). Annealing bias voltage at a set point of 3.3 V was applied by V_{ds} without a gate voltage. The suspended GNR was inspected by scanning electron microscope (SEM). As shown in Fig. 3, the suspended GNR 50 nm wide is successfully achieved by the shrink lithography.

III. Experimental Results and Discussion

A. Annealing Effect of Suspended GNR

Drain-to-source current versus gate voltage was recorded to investigate the electrical properties of the suspended GNR ISFET. Fig. 4 (a) presents the ambipolar characteristics of a GNR ISFET measured in PBS buffer solution at room temperature, showing the transition from p-type region to n-type region at the Dirac point of about 0.2 V. After applying the annealing bias voltage at a predefined set point of 3.3 V, the ambipolar behavior was enhanced, demonstrating larger intrinsic bandgap of GNR than the GNR without annealing. The enhanced ambipolar behavior after annealing is contributed by the thermal energy [22] and the suspended structure change [23] introduced by annealing. The annealing effects seem to be responsible for the larger bandgap, comparable to those of possibly much narrower ribbons [22]. The larger bandgap of GNR caused by annealing can be considered as a positive factor of enhancing ISFET sensitivity, which has been demonstrated by several other researchers [23]. As shown in Fig. 4 (b), the I-V curve of GNR ISFET were characterized in PBS buffer solution after annealing. The change of the curve slope caused by different gate voltages demonstrates the field effect.

B. pH Electrical Measurements

First, the annealed suspended GNR ISFET was used to detect different pH solutions, and compared with an unsuspended GNR and a graphene sheet in microscale under the same design, fabrication and measurement conditions. As shown in Fig. 5 (a), solutions from pH 5 to pH 9 were delivered to the suspended GNR ISFET sequentially. The electrolyte gate response of the device's drain-to-source current was measured for each solution. While the ISFET was biased at V_{ds} of 1 V, and the gate voltage from -1.8 to 1.8 V was applied. It is observed that the Dirac point of GNR shifts positively from pH 5 to pH 9. The shift of Dirac point is due to the electrostatic gating effect by introducing charged ions such as H^+ and OH^- [34]. The negative shift of Dirac point is caused by the pH decreasing. After introducing more H^+ ions, the surface of GNR was positively charged, which needed negative gate voltage to achieve a balanced condition. The suspended GNR behaves as a p-type material when negative gate potential is applied, and the I_d of the ISFET increases with the rising of pH values. On the contrary, when the gate potential is switched positive, transition from p-type region to n-type region occurs, and the I_d of the ISFET decreases with the increasing of pH.

The sensitivity of GNR ISFETs was investigated. The ISFET was biased at V_{ds} of 1 V, and the gate voltage was fixed at 1.8 V. Different solutions from pH 5 to pH 9 were introduced to the suspended GNR ISFET, unsuspended GNR ISFET and normal graphene ISFET, respectively. The width of the suspended GNR and unsuspended GNR were kept the same as 50 nm, and the normal graphene sheet was in microscale. To get a clear readout, a normalized sensitivity was deduced. I_d for pH 9 solution was used as an initial current I_0, and other I_d tested under different pH values subtracted I_0 to get ΔI. Normalized sensitivity was represented as $\Delta I/I_0$. As shown in Fig. 5 (b), the normalized sensitivity was compared among the three ISFETs, demonstrating that the suspended GNR ISFET has the best sensitivity in pH sensing. Two factors play important roles in the better sensitivity of suspended GNR, relevant to the output signal change to input signal change ratio. One factor is the suspended gap under the GNR. The hydrogen ion concentration becomes nonuniform due to the electric field present in the suspended gap [25]. Hydrogen ions will be driven to the underneath surface of the GNR by this electric field to generate larger output signals, compared with the unsuspended GNR with only one side to absorb the ions. The other one is the charge traps at the interface and in the oxide, which act as external scattering centers and degrade transport properties [26], [27], decreased greatly by suspended structure [16]. The background noise caused by the interface charge traps can be decreased, and larger magnitude of output signal can be measured.

C. PSA Measurements

Furthermore, we investigated the cancer marker detection by modifying the surface of GNR with receptor antibodies.

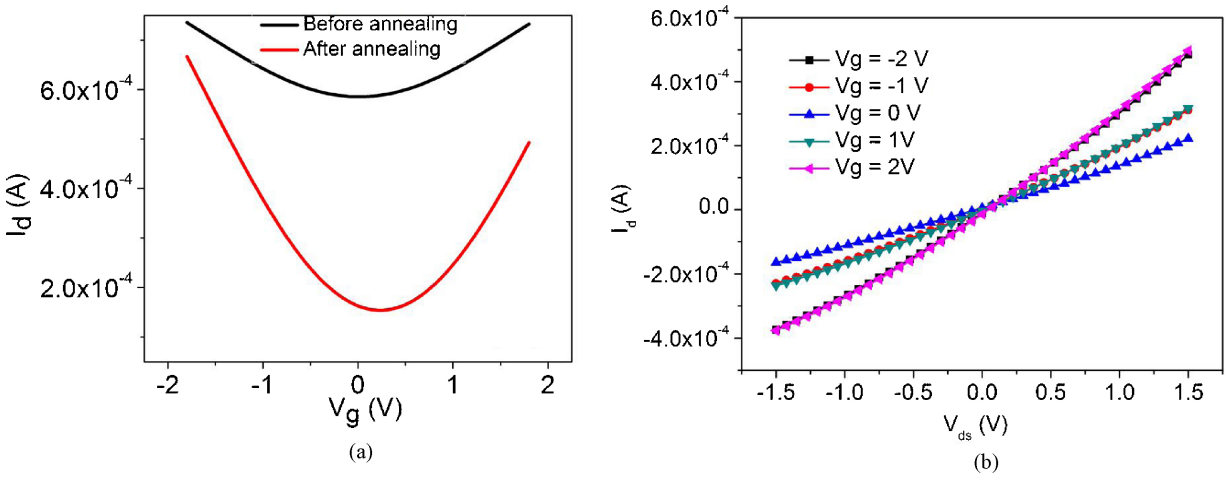

Fig. 4. (a) Ambipolar characteristics of GNR ISFET were measured in PBS buffer solution. Annealing bias voltage at a set point of 3.3 V was applied as V_{ds} without a gate voltage. The annealing process contributed the enhanced ambipolar behavior. (b) After annealing, the I–V characteristics of the GNR ISFET were measured at various gate voltages ranging from −2 to 2 V.

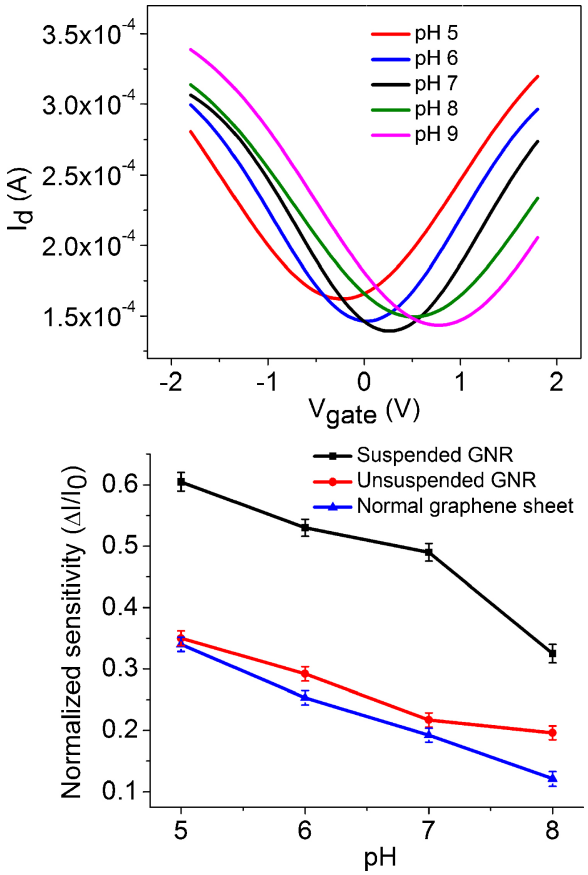

Fig. 5. (a) Ambipolar characteristics of suspended GNR ISFET in different pH solutions induced. The Dirac point of suspended GNR shifts significantly from pH 5 to pH 9. (b) Normalized sensitivities of different types of ISFET were measured. Suspended GNR presents better sensitivity than the unsuspended GNR and normal graphene. The reference pH was selected as pH 9.

Cancer biomarkers are molecules in blood or tissue, which are associated with cancer. The measurement and identification of cancer biomarker are elucidated very critical and efficient in disease prediction, diagnosis, and monitoring [28], [29]. In the meanwhile, the clinical utility of PSA to discriminate health and disease states requires the capability to detect extremely low concentration [30], which is also especially important to understand cellular processes and to search for new protein biomarkers [31]. Herein, the anti-PSA was immobilized on the surface of suspended GNR, and the ISFET was blocked with bovine serum albumin. Given that the conductance of graphene is determined by the charge carrier density and mobility, it is evident that changes in density and/or mobility of charge carriers must be responsive when molecules or ions are absorbed [32], [33]. Therefore, the conductance of the suspended GNR modified with the PSA capture antibody shifts as the concentration change of PSA solutions.

As shown in Fig. 6 (a), different concentrations of PSA from 0–4 ng/mL were introduced to surface modified suspended GNR ISFET sequentially. The ambipolar characteristics of suspended GNR ISFET was measured at different PSA solutions. The ISFET was biased at V_{ds} of 1 V, and the gate voltage was applied from −1.8 to 1.8 V. After fixing the gate voltage and the drain-source voltage, the drain current, I_d, would increase with the concentration of PSA. There is small right shift of the Dirac point of suspended GNR from 0 to 4 ng/mL PSA solution, which is much less shift compared with pH detection. The shift of Dirac point is due to the electrostatic gating effect by adsorbed charge species [34]. The positive shift of Dirac point is caused by the negative charges of the adsorbed PSA which can only be balanced by positive gate voltage. However, the interaction between GNR and PSA immunoreaction bonding is relative weak compared to the H^+. Therefore, the positive shift of Dirac point is not obvious, and conductance change becomes dominant.

The sensitivity of the different ISFETs was also investigated for the PSA detection. The ISFET was biased at V_{ds} of 1 V, and the gate voltage was fixed at 1.8 V. Different concentrations of PSA solutions from 0 ng/mL to 4 ng/mL were introduced to the suspended GNR, unsuspended GNR and microscale graphene ISFETs, respectively. Normalized sensitivity was introduced as follow: I_d for PBS solution containing no PSA was used as an initial conductance I_0, and other I_d tested under different concentrations of PSA solutions subtracted I_0 to get ΔI. Normalized sensitivity was represented as $\Delta I/I_0$.

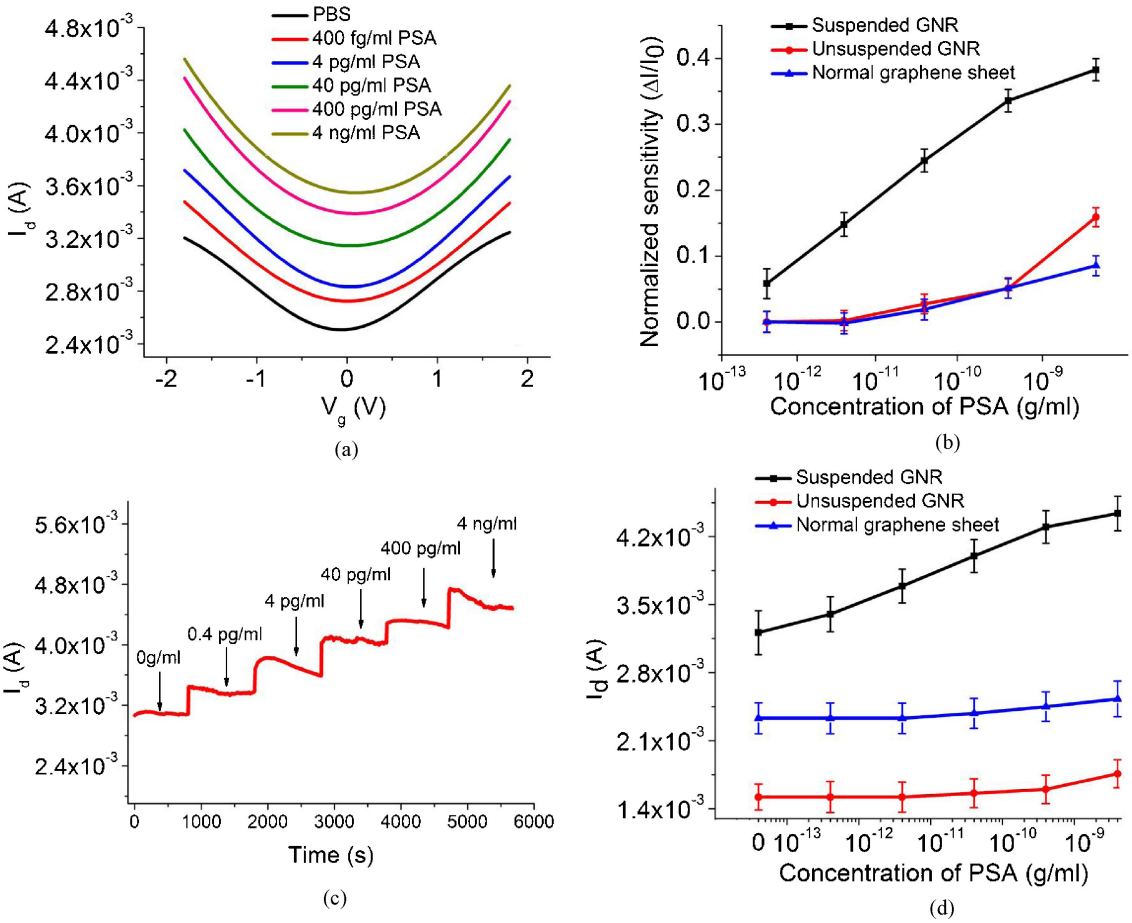

Fig. 6. (a) Ambipolar characteristics of suspended GNR ISFET with different PSA solutions induced. The Dirac point of suspended GNR does not shift as significantly as pH detection. (b) Normalized sensitivities of different types of ISFETs were measured. Suspended GNR presents the best sensitivity. PBS solution contain no PSA was selected as the reference solution. (c) Real-time current change while the different concentrations of PSA solutions were provided to the suspended GNR sensor (d) Drain-to-source current versus different PSA concentrations were recorded for different types of ISFET. The results demonstrate that the detection limit of suspended GNR is down to 0.4 pg/mL, compared with the unsuspended GNR and normal graphene with a detection limit of 40 pg/mL.

As shown in Fig. 6 (b), the normalized sensitivities were compared among the three types of ISFET, demonstrating that suspended GNR ISFET has best sensitivity performance in cancer biomarker sensing.

In addtion, the detection limit of different types of ISFET was also investigated. As shown in Fig. 6(c), the real-time current change was recorded while the different concentrations of PSA solutions were introduced to the suspended GNR sensor. As shown in Fig. 6 (d), different concentrations of PSA were delivered to the three ISFETs. The detection limit of suspended GNR ISFET was 0.400 pg/mL, but the unsuspended GNR and microscale normal graphene ISFETs were 40 pg/mL. The signal-to-noise ratio plays a very important role in the enhancement of detection limit of ISFET. The current power spectra can be expressed as $S_I = AI^2 f^{\beta}$, where S_I is the noise power density, I is current, f is the frequency, A is defined as the 1/f noise amplitude, and β is the frequency exponent with a value close to -1 [35]. It was reported that trapped charges at the interface and in the substrate degrade transport characteristics of a single-layer graphene [16], which exhibits the effect in our experiment results.

The specificity of the suspended GNR ISFET was also studied by three control experiments. First, different concentrations of PSA were delivered to suspended GNR without any modification, and the drain-to-source current was recorded when the ISFET was biased at V_{ds} of 1 V, and the gate voltage was applied at 1.8 V. As shown in Fig. 7, the I_d kept constant, demonstrating bare GNR did not absorb PSA. Next, under the same V_{ds} and V_g, the suspended GNR with goat anti-rabbit IgG modified was used to detect different concentrations of PSA solutions. The I_d of GNR kept constant. In addition, the non-specific reaction of normal rabbit IgG was also implemented to prove the specificity of this suspended GNR functionalized with PSA capture antibodies. The modification of antirabbit IgG process was described in our previous report [36].

IV. Conclusion

In summary, the fabrication of suspended GNR ISFET using shrink lithography was investigated, making the nanolithography cost effective due to the inexpensive thermoplastics and molding process. The pH sensing was characterized based on

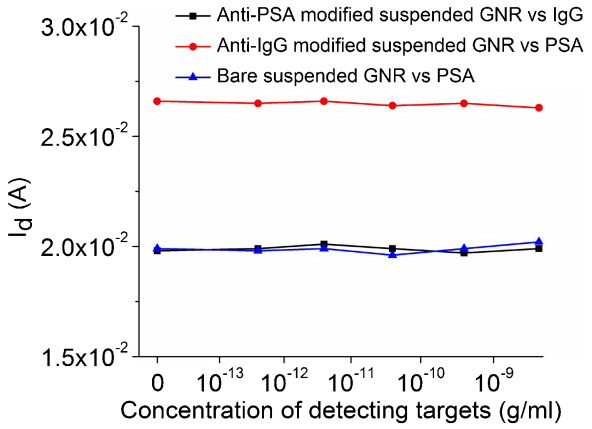

Fig. 7. Different concentrations of PSA were introduced to suspended GNR without any modification and with anti-IgG modification. Different concentrations of normal rabbit IgG were introduced to suspended GNR with anti-PSA modification. And the drain-to-source current was recorded when the ISFET was biased at V_{ds} at 1 V, and the gate voltage was applied at 1.8 V. The I_d kept constant.

the suspended GNR ISFET to show positive shift of the Dirac point with the increase of pH. PSA was also detected with bioreceptors. The detection limit of suspended GNR ISFET for PSA detection is down to 0.4 pg/mL. Annealing effect on the ambipolar characteristics of suspended GNR was also investigated. In comparison, unsuspended GNR and microscale graphene sheets based ISFETs were characterized, showing that suspended GNR ISFET was superior in sensitivity and detection limit. Moreover, this low-cost detection platform can be extended to the recognition of other antigens, which may open a way to diagnose other cancer and diseases.

ACKNOWLEDGMENT

The authors would like to thank the Nanofabrication Center and the Characterization Facility at the University of Minnesota for assistance with fabrication and characterization.

REFERENCES

[1] X. Wang and H. Dai, "Etching and narrowing of graphene from the edges," *Nat. Chem*, vol. 2, no. 8, pp. 661–665, 2010.
[2] X. Li, X. Wang, L. Zhang, S. Lee, and H. Dai, "Chemically derived, ultrasmooth graphene nanoribbon semiconductors," *Science*, vol. 319, no. 5867, pp. 1229–1232, 2008.
[3] D. V. Kosynkin, A. L. Higginbotham, A. Sinitskii, J. R. Lomeda, A. Dimiev, B. K. Price, and J. M. Tour, "Longitudinal unzipping of carbon nanotubes to form graphene nanoribbons," *Nature*, vol. 458, no. 7240, pp. 872–877, 2009.
[4] L. Tapasztó, G. Dobrik, P. Lambin, and lá szló P. Biró, "Tailoring the atomic structure of graphene nanoribbons by scanning tunnelling microscope lithography," *Nat. Nanotech*, vol. 3, no. 7, pp. 397–401, 2008.
[5] L. Jiao, L. Zhang, L. Ding, J. Liu, and H. Dai, "Aligned graphene nanoribbons and crossbars from unzipped carbon nanotubes," *Nano Res*. vol. 3, no. 6, pp. 387–394, 2010.
[6] Z. Zhang, Z. Sun, J. Yao, D. V. Kosynkin, and J. M. Tour, "Transforming carbon nanotube devices into nanoribbon devices," *J. Amer. Chem. Soc*. vol. 131, no. 37, pp. 13460–13463, 2009.
[7] A. L. Higginbotham, D. V. Kosynkin, A. Sinitskii, Z. Sun, and J. M. Tour, "Lower-defect graphene oxide nanoribbons from multiwalled carbon nanotubes," *ACS Nano*, vol. 4, no. 4, pp. 2059–2069, 2010.
[8] H. Santos, L. Chico, and L. Brey, "Carbon nanoelectronics: Unzipping tubes into graphene ribbons," *Phys. Rev. Lett*. vol. 103, no. 8, 086801, 2009.
[9] S. Zhang, S. Tang, J. Lei, H. Dong, and H. Ju, "Functionalization of graphene nanoribbons with porphyrin for electrocatalysis and amperometric biosensing," *J. Electroanal. Chem*., vol. 656, nos. 1–2, pp. 285–288, 2011.
[10] K. R. Ratinac, W. Yang, S. P. Ringer, and F. Braet, "Toward ubiquitous environmental gas sensorssCapitalizing on the promise of graphene," *Environ. Sci. Technol*., vol. 44, no. 4, pp. 1167–1176, 2010.
[11] L. Liu, Y. Zhang, W. Wang, C. Gu, X. Bai, and E. Wang, "Nanosphere lithography for the fabrication of ultranarrow graphene nanoribbons and on-chip bandgap tuning of graphene," *Adv. Mat*., vol. 23, no. 10, pp. 1246–1251, 2011.
[12] G. Liu, Y. Wu, Y. Lin, D. B. Farmer, J. A. Ott, J. Bruley, A. Grill, P. Avouris, D. Pfeiffer, A. A. Balandin, and C. Dimitrakopoulos, "Epitaxial graphene nanoribbon array fabrication using BCP-assisted nanolithography," *ACS Nano*., vol. 6, no. 8, pp. 6786–6792, 2012.
[13] Y. Huang, X. Dong, Y. Shi, C. M. Li, L. Li, and P. Chen, "Nanoelectronic biosensors based on CVD grown graphene," *Nanoscale*, vol. 2, pp. 1485–1488, Apr. 2010.
[14] H. G. Sudibya, Q. He, H. Zhang, and P. Chen, "Electrical detection of metal ions using field-effect transistors based on micropatterned reduced graphene oxide films," *ACS Nano*. vol. 5, no. 3, pp. 1990–1994, 2011.
[15] X. Dong, Y. Shi, W. Huang, P. Chen, and L. Li, "Electrical detection of DNA hybridization with single-base specificity using transistors based on CVD-grown graphene sheets," *Adv. Mat*. vol. 22, no. 14, pp. 1649–1653, 2010.
[16] Z. Cheng, Q. Li, Z. Li, Q. Zhou, and Y. Fang, "Suspended graphene sensors with improved signal and reduced noise," *Nano. Lett*, vol. 10, no. 5, pp. 1864–1868, 2010.
[17] X. Zhao, Y. Xia, O. Schueller, D. Qin, and G. Whitesides, "Fabrication of microstructures using shrinkable polystyrene films," *Sens. Actuators A*, vol. 65, nos. 2–3, pp. 209–217, 1998.
[18] D. Dyer, S. Shreim, S. Jayadev, V. Lew, E. Botvinick, and M. Khine, "Sequential shrink photolithography for plastic microlens arrays," *Appl. Phys. Lett*. vol. 99, no. 3, 034102, 2011.
[19] P. Li, Z. You, G. Haugstad, and T. Cui, "Graphene fixed-end beam arrays based on mechanical exfoliation," *Appl. Phys. Lett*, vol. 98, no. 25, 253105, 2011.
[20] M. Lu, D. Lee, W. Xue, and T. Cui, "Flexible and disposable immunosensors based on layer-by-layer self-assembled carbon nanotubes and biomolecules," *Sens. Actuators A*, vol. 150, no. 2, pp. 280–285, 2009.
[21] L. Hua, X. Wu, and R. Wang, "Glucose sensor based on an electrochemical reduced graphene oxide-poly-(L-Lysine) composite film modified GC electrode," *Analyst*, vol. 137, no. 24, pp. 5716–5719, 2012.
[22] T. Shimizu, J. Haruyama, D. C. Marcano, D. V. Kosinkin, J. M. Tour, K. Hirose, and K. Suenaga, "Large intrinsic energy bandgaps in annealed nanotube-derived graphene nanoribbons," *Nat. Nanotech*., vol. 6, pp. 45–50, Jan. 2010.
[23] M. Lin, C. Ling, Y. Zhang, H. J. Yoon, M. M. Cheng, L. A. Agapito, N. Kioussis, N. Widjaja, and Z. Zhou, "Room-temperature high on/off ratio in suspended graphene nanoribbon field-effect transistors," *Nanotechnology*, vol. 22, no. 26, 265201, 2011.
[24] H. Cheng, C. Wu, P. Hsu, C. Wang, T. Liao, and Y. Wu, "High sensitivity of dry-type nanowire sensors With high-k Dielectrics for pH detection via capillary atomic force microscope tip coating technique," *IEEE Electron Device Lett.*, vol. 33, no. 9, pp. 1312–1314, 2012.
[25] F. Bendriaa, F. Le Bihan, A. C. Salaün, T. Mohammed-Brahim, and O. Bonnaud, "Highly sensitive suspended-gate ion sensitive transistor for the detection of pH," in *Proc. SPIE*, vol. 5866, Jul. 2005, pp. 433–440.
[26] Y. Lin and P. Avouris, "Strong suppression of electrical noise in bilayer graphene nanodevices," *Nano. Lett*., vol. 8, no. 8, pp. 2119–2125, 2008.
[27] G. Liu, W. Stillman, S. Rumyantsev, Q. Shao, M. Shur, and A. A. Balandin, "Low-frequency electronic noise in the double-gate single-layer graphene transistors," *Appl. Phys. Lett*., vol. 95, no. 3, 033103, 2009.
[28] R. Etzioni, N. Urban, S. Ramsey, M. McIntosh, S. Schwartz, B. Reid, J. Radich, G. Anderson, and L. Hartwell, "The case for early detection," *Nat. Rev*., vol. 3, no. 4, pp. 1–10. 2003.
[29] Z. Zhong, W. Wu, D. Wang, D. Wang, J. Shan, Y. Qing, and Z. Zhang, "Nanogold-enwrapped graphene nanocomposites as trace labels for sensitivity enhancement of electrochemical immunosensors in clinical immunoassays: carcinoembryonic antigen as a model," *Biosens. Bioelectron*, vol. 25, no. 10, pp. 2379–2383, 2010.

[30] H. Lilja, D. Ulmert, and A. J. Vickers, "Prostate-specific antigen and prostate cancer: Prediction, detection and monitoring," *Nat. Rev.*, vol. 8, no. 4, pp. 268–278, 2008.
[31] L. A. Tessler, J. G. Reifenberger, and R. D. Mitra, "Protein Quantification in Complex Mixtures by Solid Phase Single-Molecule Counting," *Anal. Chem*. vol. 81, no. 17, pp. 7141–7148, 2009.
[32] E. H. Hwang, S. Adam, and S. Das Sarma, "Transport in chemically doped graphene in the presence of adsorbed molecules," *Phys. Rev. B*, vol. 76, no. 19, 195421, 2007.
[33] F. Schedin, A. K. Geim, S. V. Morozov, E. W. Hill, P. Blake, M. I. Katsnelson, and K. S. Novoselov, "Detection of individual gas molecules adsorbed on graphene," *Nat. Mat.*, vol. 6, no. 9, pp. 652–655, 2007.
[34] I. Heller, A. M. Janssens, J. Ma1nnik, E. D. Minot, S. G. Lemay, and C. Dekker, "Identifying the mechanism of biosensing with carbon nanotube transistors," *Nano Lett.*, vol. 8, no. 2, pp. 591–595, 2008.
[35] Y. Lin, J. Appenzeller, J. Knoch, Z. Chen, and P. Avouris, "Low-frequency current fluctuations in individual semiconducting single-wall carbon nanotubes," *Nano Lett.*, vol. 6, no. 5, pp. 930–936, 2006.
[36] B. Zhang and T. Cui, "An ultrasensitive and low-cost graphene sensor based on layer-by-layer nano self-assembly," *Appl. Phys. Lett.*, vol. 98, no. 7, 073116, 2011.

Bo Zhang received the B.S. degree from the Department of Precision Instruments and Mechanology, Tsinghua University, Beijing, China, in 2009. He is currently pursuing the Ph.D. degree in the Department of Mechanical Engineering, University of Minnesota.

His current research interests include micro/nano fabrication technologies, biosensors, polymer microelectronics, and solar systems.

Tianhong Cui (M'04–SM'04) received the B.S. degree from the Nanjing University of Aeronautics and Astronautics, Nanjing, China, in 1991, and the Ph.D. degree from the Chinese Academy of Sciences, Beijing, China.

He is currently a Professor of mechanical engineering with the University of Minnesota. His current research interests include MEMS/NEMS, nanotechnology, and polymer electronics.